Nuclear Instruments and Methods in Physics Research A 733 (2014) 226–232

Contents lists available at ScienceDirect

Nuclear Instruments and Methods in Physics Research A

journal homepage: www.elsevier.com/locate/nima

The NDCX-II engineering design

W.L. Waldron [a,*], W.J. Abraham [a], D. Arbelaez [a], A. Friedman [b], J.E. Galvin [a], E.P. Gilson [c], W.G. Greenway [a], D.P. Grote [b], J.-Y. Jung [a], J.W. Kwan [a], M. Leitner [a,1], S.M. Lidia [a], T.M. Lipton [a], L.L. Reginato [a], M.J. Regis [a], P.K. Roy [a], W.M. Sharp [b], M.W. Stettler [a], J.H. Takakuwa [a], J. Volmering [a], V.K. Vytla [a]

[a] Lawrence Berkeley National Laboratory, Berkeley, CA 94720, USA
[b] Lawrence Livermore National Laboratory, Livermore, CA 94550, USA
[c] Princeton Plasma Physics Laboratory, Princeton, NJ 08543, USA

ARTICLE INFO

Available online 7 June 2013

Keywords:
Induction accelerator
High energy density laboratory physics
Heavy ion fusion

ABSTRACT

The Neutralized Drift Compression Experiment (NDCX-II) is a user facility located at Lawrence Berkeley National Laboratory which is uniquely designed for ion-beam-driven high energy density laboratory physics and heavy ion fusion research. Construction was completed in March 2012 and the facility is now in the commissioning phase. A significant amount of engineering was carried out in order to meet the performance parameters required for a wide range of target heating experiments while making the most cost-effective use of high-value hardware available from a decommissioned high current electron induction accelerator. The technical challenges and design of this new ion induction accelerator facility are described.

1. Introduction

Ion beams can be used to pulse-heat target materials for high energy density laboratory physics (HEDLP) experiments and as drivers for inertial fusion energy (IFE) targets [1,2]. In contrast with laser beams, which deposit their energy onto the surface of a target, ion beams deposit their energy into the volume of the target material. By heating a target foil with an ion beam near the Bragg peak energy (the peak of the stopping power curve dE/dX), there can be both efficient energy transfer as well as highly uniform energy deposition [3]. Even at energies below the Bragg peak, volumetric energy deposition is a valuable property which can be exploited for a variety of target heating experiments [4].

The first phase of the Neutralized Drift Compression Experiment (NDCX-I) has successfully demonstrated simultaneous radial and longitudinal beam compression using a technique of imparting a velocity ramp on the ion beam, letting the beam drift through a neutralizing plasma to offset space-charge forces, and applying a strong solenoidal field before the target [5,6]. To provide sufficient energy deposition over a time duration which is comparable to the hydrodynamic expansion time, neutralized drift compression has been developed to produce ~1 ns, ~1 mm diameter beams from much longer beams with modest energy. NDCX-I has provided a beam for initial target experiments and diagnostic development [7]. The second phase of the Neutralized Drift Compression Experiment (NDCX-II) has been developed with increased beam energy to probe the warm dense matter regime (WDM) at higher temperatures and pressures.

The NDCX-II facility shown in Fig. 1 is centered around an ion induction accelerator at Lawrence Berkeley National Laboratory (LBNL) designed to pulse-heat target materials to study the state and evolution of the materials with fast diagnostics. The $11 M NDCX-II construction project was completed in March 2012 and the facility is now in the commissioning phase. In 2013, when initial experiments begin, the commissioned facility will transition to a user facility for HEDLP, IFE, and intense-beam research.

2. Accelerator design

The NDCX-II physics design was developed based on the experience from NDCX-I in longitudinal and radial beam compression in a neutralizing plasma and designed to make maximum use of the available induction cells and pulsed power systems from the decommissioned Advanced Test Accelerator (ATA) [8,9,10]. Whereas NDCX-I has a single induction gap for applying the compression voltage waveform before the neutralizing plasma drift line, NDCX-II includes a series of gaps which provide a flexible platform for applying multiple stages of compression and acceleration using mature technology from ATA. The nominal beamline configuration shown in Fig. 2 includes an injector, active

* Corresponding author.
E-mail address: WLWaldron@lbl.gov (W.L. Waldron).
[1] Now at Michigan State University.

0168-9002/$ - see front matter © 2013 Elsevier B.V. All rights reserved.
http://dx.doi.org/10.1016/j.nima.2013.05.063

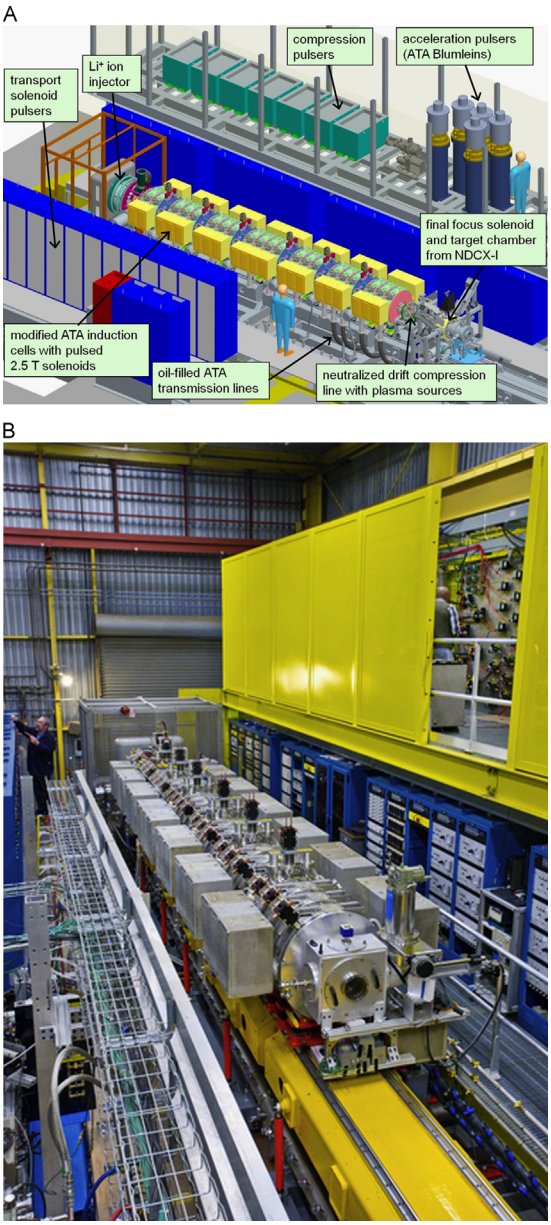

Fig. 1. NDCX-II facility CAD model and picture.

induction cells, inactive induction cells, diagnostic cells, and a neutralizing plasma drift line. The source-to-target distance is approximately 10 m. All cells have transport solenoids for radial focusing, but only the active induction cells are driven with high voltage pulsed power systems and apply carefully tailored compression and acceleration voltage waveforms to the beam. Inactive cells provide drift space for the beam to longitudinally compress after a velocity tilt has been imposed by an active cell via a ramped voltage waveform. Because the inactive cells are physically equivalent to the active cells, multiple beamline configurations can be considered that also utilize these locations for compression and acceleration. A significant fraction of the accelerator is dedicated to non-neutralized longitudinal compression of the beam.

To extract a total charge of 50 nC from the ion source, the flattop pulse duration at the injector is approximately 600 ns. To use the limited volt-seconds of the induction cells for high gradient acceleration and take advantage of the Blumlein pulsed power systems from ATA, the beam pulse duration must first be compressed to less than 70 ns. A final velocity tilt is applied at the end of the accelerator before the beam enters the neutralized drift section, where a volumetric plasma is created with sufficient density to cancel the beam's space charge defocusing force and enable final compression to less than 1 ns and a mm scale focal spot at the target. The short beam duration allows energy deposition over a timescale comparable to the hydrodynamic expansion time of the target [4]. The shot rate for the facility is 1 shot per 30 s and is limited by the cooling of the pulsed transport solenoids operating at 2.5 T. Beam parameters based on particle-in-cell simulations are shown in Table 1.

3. Injector and ion source

Because of the desire for an appropriate ion range at energy levels of 1–4 MeV and the resident expertise in fabricating large diameter thermionic alumino-silicate ion sources, lithium was chosen for NDCX-II. These ion sources can produce low emittance and high charge purity beams [11]. For an aluminum target, lithium has a Bragg peak at 1.9 MeV. For the most uniform energy deposition, the beam should enter the target foil with an energy slightly above the Bragg peak so that the beam energy is at the Bragg peak when reaching the center of the foil. Testing of smaller area sources achieved 1 mA/cm^2 space-charge limited current density at 1275 °C [12]. To produce the desired 50 nC, the ion source diameter for the NDCX-II injector is 10.9 cm and the extracted current flattop pulse duration is approximately 600 ns. The large surface area at high operating temperature generates significant power loss to radiation from the ion source assembly which requires approximately 4 kW of heating power (~60 V,~65 A). The temperature of the heater filament approaches 2000 °C and precludes the use of a conventional filament potted in alumina. The filament must be electrically isolated from the tungsten housing and requires the use of high temperature boron nitride insulators (Fig. 3). For maintenance considerations, the injector is designed to allow easy access to the source assembly through the high voltage dome inside the ground cage. The 40–80 h lifetime of the filament is currently the limiting factor in continuous daily injector operation. Improving source lifetime, emission current density, and filament lifetime are parts of an ongoing research and development effort [13].

The beam extraction geometry is shown in Fig. 4 and includes an ion source pulsed to +130 kV by a spark gap switched pulse forming network followed by a 1:5 step-up autotransformer with an active reset circuit (Fig. 5). A parallel resistor and inductor network in series with the PFN output can be used to adjust the pulse flattop. This feature can be used to compensate for transformer voltage droop or to apply a ramped voltage waveform for bunching. There is also a resistive voltage divider on the transformer output which allows the use of a lower voltage tap for the extraction electrode. The acceleration electrode is driven with a DC power supply. Power to the ion source heater filament is provided through a 60 Hz 1:1 isolation transformer. For thermal management, electrodes near the ion source are water cooled. A 2.5 T pulsed solenoid magnet with dipole steering magnets is located at the injector exit, upstream of the first induction cell. The original injector design contained a segmented Rogowski coil to measure the beam current and centroid. After initial testing found the signal-to-noise ratio to be too low, the Rogowski coil was replaced with a conventional current transformer. Because the core of the current transformer saturates when using the pulsed solenoid, this diagnostic is only useful to quantify the beam current out of the injector when the first transport solenoid is not energized.

The injector hardware is shown in Fig. 6 and includes a graded alumina ceramic insulator with an inner diameter of 65 cm to enclose the system and provide enough room for thermal

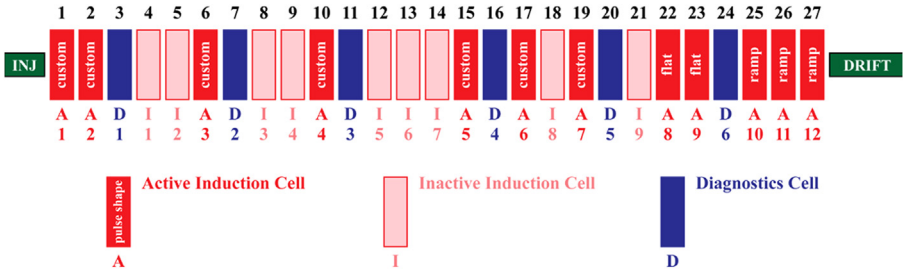

Fig. 2. Nominal beamline configuration of NDCX-II.

Table 1
NDCX-II beam parameters at the target plane from WARP simulations of the 27 cell configuration (12 active cells).

Ion species	Li^+ (A=7)
Total extracted charge	50 nC
Ion kinetic energy	1.2 MeV
Focal radius (containing 50% of beam)	0.6 mm
Bunch duration (FWHM)	0.6 ns
Peak current	36 A
Charge within the final compressed pulse	30 nC
Peak energy fluence (time integrated over entire beam)	8.6 J/cm^2
Fluence within 0.1 mm diameter spot and FWHM duration	5.3 J/cm^2

management [14]. This large diameter insulator was reused from a previous ion source test stand and is composed of epoxied ceramic rings [15]. The stack of insulators is held in compression with 8 Torlon 4203 rods. There is also a custom resistive voltage divider to monitor the pulsed voltage applied to the high voltage dome and ion source assembly.

Although the additional vacuum loading of the epoxy is not ideal, a new brazed ceramic insulator stack was estimated at $500 k with an 8 month delivery time, which was deemed prohibitive. Outgassing tests were performed on the epoxy at the expected temperature to ensure that the vacuum load was acceptable. The injector base pressure at ambient temperature is in the low 10^{-6} Torr range and rises to the low 10^{-5} Torr range at the working temperature.

4. Accelerator cells

The NDCX-II accelerator cell design is based on the design of the ATA induction cells, but significant modifications were made to meet the requirements of NDCX-II (Fig. 7). To provide more room for the high field pulsed solenoids and to reduce the axial extent of the fringe fields (and thus shorten the required voltage pulses by reducing the ion transit time), the acceleration gap geometry was changed by reducing the beam pipe radius from 6.72 cm to 3.97 cm. The 0.3 T DC water cooled solenoids from ATA were replaced with 2.5 T pulsed solenoids to transversely confine the NDCX-II ion beam (Fig. 8). To prevent the return flux due to the pulsed solenoid from saturating a significant fraction of the ferrite toroids, a copper cylinder was placed between the solenoid OD and the ferrite ID. Cell flanges were also thinned to reduce eddy currents and inhibit the directing the solenoid magnetic field into the ferrite toroids. The original porcelain insulators from ATA were replaced with Rexolite 1422 insulators, which have been used in other induction accelerators [16,17,18]. Rexolite has a lower dielectric constant than porcelain which lowers the electric field enhancement at dielectric interfaces. Although Rexolite has a higher vacuum outgassing rate than porcelain, there was concern about the porcelain being brittle and creating the risk of a catastrophic failure under mechanical stress.

Since the NDCX-II ion beam has a large energy spread associated with the rapid pulse compression, misalignment of the solenoids leads to corkscrew deformation of the beam and reduced intensity at focus [19,20]. Therefore, precise alignment of the solenoids with respect to the accelerator axis is critical. The pulsed wire method was chosen to characterize the magnetic axis of the pulsed solenoids [21]. This method has the advantage that the location of the wire, once aligned, naturally defines the magnetic axis. Furthermore, the method can be applied to pulsed solenoids by timing the current pulse on the wire such that it occurs at the peak of the magnet pulse. When a short current pulse is passed through the wire, the Lorentz force generates a mechanical disturbance. This disturbance then propagates along the wire and is measured with an optical detector. The wire motion signature (as a function of time) is proportional to the integral of the magnetic field (as a function of distance), where the distance and time coordinates are related through the speed of wave propagation. Since tilt and offset misalignments produce wire motion signatures that can be differentiated from one another, the alignment of the wire with the magnetic axis is straight forward. Once the wire is aligned with the solenoid's magnetic axis, its position can be related to fiducial points on the solenoid. This is accomplished by using a laser tracker along with calibrated laser micrometers, which are used to determine the location of the wire.

For the alignment of the accelerator, adjustment screws on the cells are first used to ensure that the front and back flanges of the cells are parallel to one another. A preliminary fiducialization of the cell is then performed based on mechanical features. The solenoids are then aligned within the cell using eight wedge/screw mechanisms in order to minimize tilt and offset errors before welding the cell closed. After welding the solenoids into the cell, the offset errors are typically less than 200 μm, while the tilt errors are typically below 1 mrad. It is critical that the tilt errors (i.e. parallelism error between the solenoid and cell axis) are small after this step. However, offset errors are less critical at this point since the transverse position of the cells can be adjusted after they are installed on the girders. With the wire aligned with the magnetic axis of the welded cell, a final fiducialization is performed that relates the magnetic axis of the cell to its external fiducials. Once the cells are placed on the girders, the fiducial information is used to set their transverse position. The angular alignment accuracy is set by the tilt errors of the solenoids (typically < 1 mrad) and the parallelism of the cell (typically < 0.1 mrad). Although no solenoid movement is expected after welding the assembly into the cell, the alignment of an individual solenoid with respect to fiducials on the cell housing can be rechecked offline with the pulsed wire method. There is also the possibility of implementing a pulsed wire alignment check of solenoids in cells while still on the beamline.

5. Pulsed power systems for accelerator cells

The high current pulsers to drive the solenoids are thyristor-switched capacitors with reverse voltage protection for the

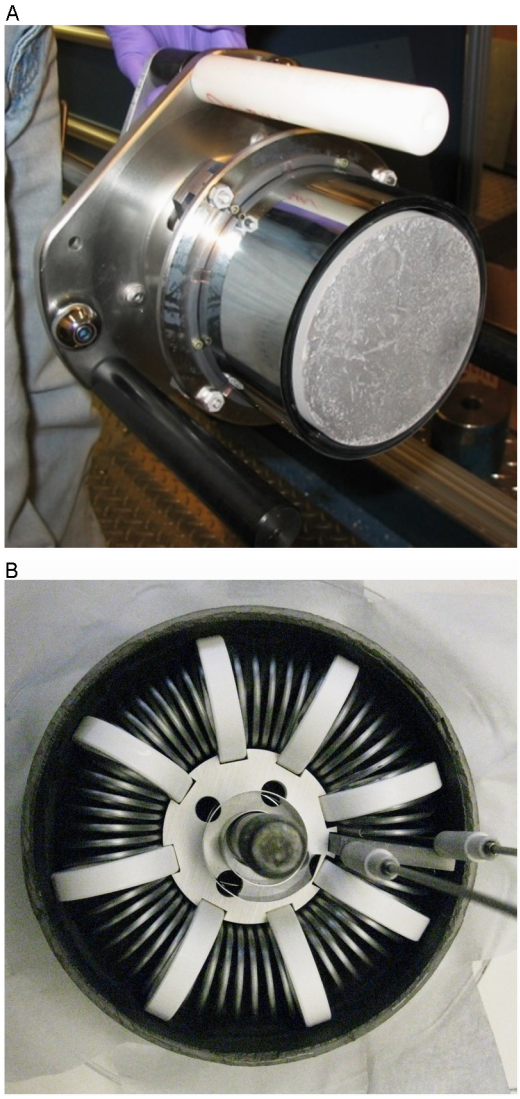

Fig. 3. Ion source assembly (top image) and filament assembly (bottom image).

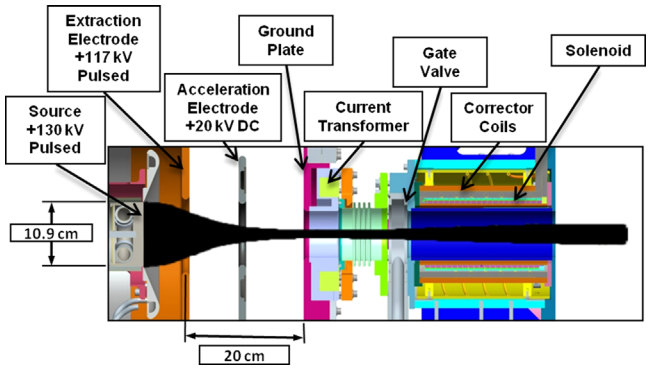

Fig. 4. Injector components and beam extraction geometry for the NDCX-II injector. The simulated beam envelope is illustrated in black.

charging power supply and a snubber network across the output to limit the amplitude of voltage transients during thyristor recovery at the end of the current pulse [22]. For 2.5 T operation, a charge voltage of 3 kV is required to produce a 2.4 ms half-sinusoid current waveform with a peak of 7 kA. Because of the low repetition rate, there is no energy recovery. At the end of the current pulse, the reverse voltage on the capacitor is dissipated in a resistor array.

The compression pulsers which drive the first seven active induction cells are custom spark gap switched lumped element circuits which are tuned to produce the required cell voltage waveforms. The tuning of these waveforms is also performed by changing circuit components in the compensation boxes where the high voltage feed comes into the induction cell. The ideal waveforms from the physics design, shown in Fig. 9, were derived using the 0.0175 V-second limit of the TDK PE11B ferrite in the ATA induction cell via detailed simulations [9,20,23]. There are active reset circuits to maximize the available magnetic flux swing from the ferrite cores. With the exception of the first pulser which is optionally used at very low voltage to equalize the beam energy out of the injector, the usable peak voltage range is 30–90 kV and the ramp duration range is 300–700 ns. Initial cell voltage waveforms produced by the compression pulsers for active cells 1–7 are shown in Fig. 10.

The Blumleins from ATA which drive the last 5 active induction cells of the baseline configuration were cleaned and some damaged cast epoxy insulators were replaced with Rexolite 1422. The only modification to the system was changing the thyratron switched charging chassis so that it could be charged from a DC power supply instead of the ATA command-resonant-charging system. The timing jitter of the compression pulsers and the Blumleins is 2–3 ns (rms). Measured Blumlein output voltage waveforms are shown in Fig. 11. These waveforms were used directly in the physics simulations. The flattop waveform with 70 ns FWHM duration is generated by matching the load impedance to the 12 Ω impedance of the Blumlein while the ramped voltage waveform is produced by capacitively loading the Blumlein at the compensation box where the high voltage feed comes into the induction cell [24].

6. Diagnostic cells

There are six dedicated diagnostic cells which also serve as vacuum pumping stations. Each diagnostic cell contains a transport solenoid, a pair of dipole steering magnets, and a set of four capacitively-coupled beam position monitors (Fig. 12). The beam position monitors are actually attached to the accelerator cell just upstream of the diagnostic cell and the signal cables are routed through dedicated ports on the diagnostic cell. The solenoids and their pulsers are the same as the ones used for the accelerator cells except that the solenoid is housed in a vacuum tight stainless steel enclosure. The dipole steering magnets are driven with an electrolytic capacitor bank and an H-bridge configuration of insulated gate bipolar transistors (IGBT's) so that the polarity of the output current can be remotely switched. The maximum peak dipole field is approximately 300 G. A diagnostic cell upgrade plan has been developed to implement the retraction of the solenoid assembly in order to allow the insertion of intercepting beam diagnostics at any of the diagnostic cell locations along the beamline. The concept is that the solenoid assembly is pressed against kinematic mounts and is supported by a motor driven actuator which can move the solenoid assembly axially off of the kinematic mounts, and then move the assembly vertically out of the beam's path, making room for an intercepting beam diagnostic without breaking vacuum. A vacuum gate valve operates in a similar fashion. The prototyping phase of this upgrade activity will have to demonstrate sufficient accuracy and repeatability. To monitor the beam current longitudinal profile along the accelerator, the inactive induction cells are

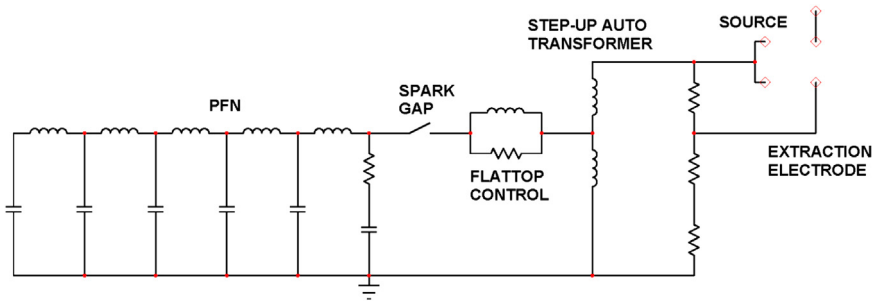

Fig. 5. Simplified schematic of the injector pulser.

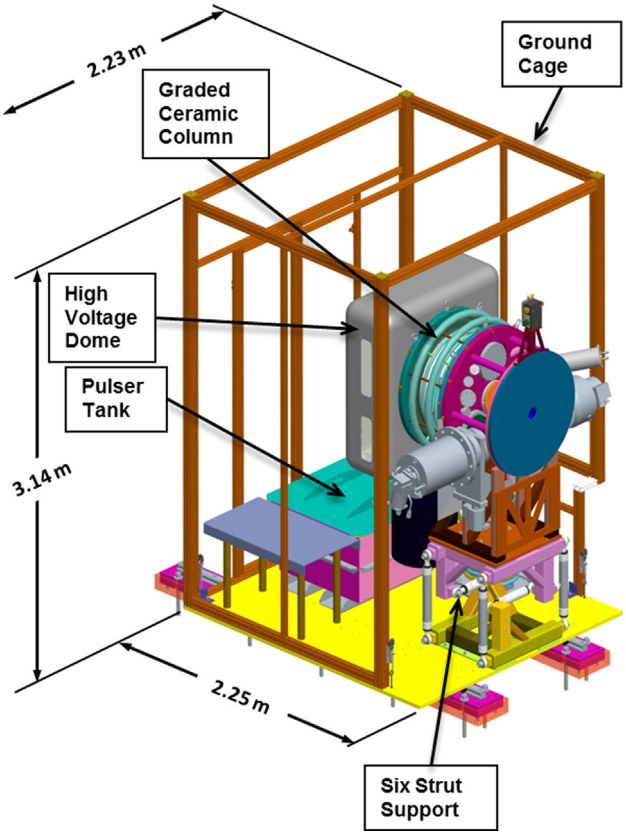

Fig. 6. NDCX-II injector.

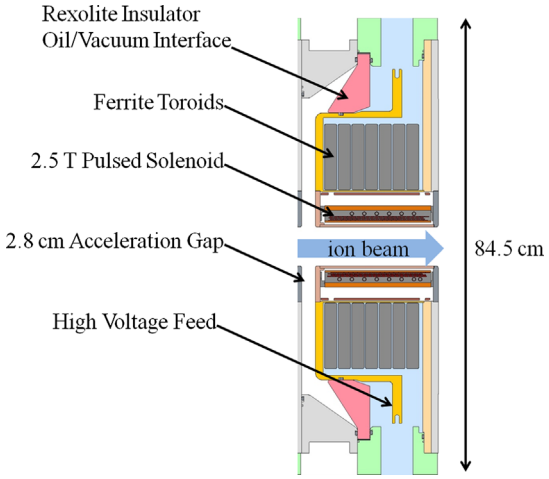

Fig. 7. NDCX-II induction cell.

Fig. 8. 2.5 T pulsed solenoid assembly enclosed by a copper cylinder in the upper image to keep the magnetic field from entering the ferrite and an induction cell in the lower image showing the solenoid position before welding into place.

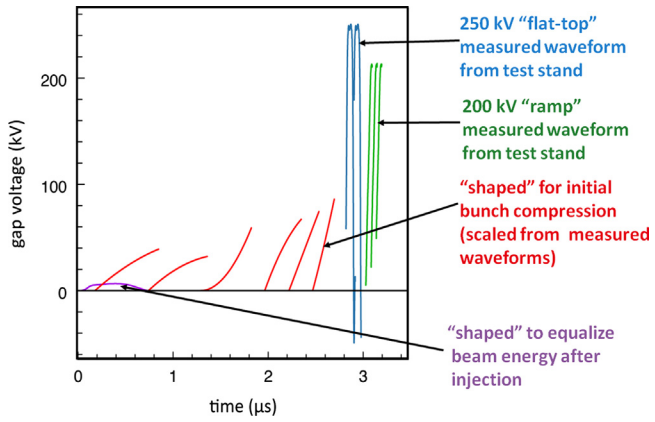

Fig. 9. Ideal compression pulser and Blumlein voltage waveforms for the 12 active cells of the baseline configuration. Note that the actual pulser outputs are negative with respect to ground and are applied to the cell high voltage feeds to accelerate the positively charged ions.

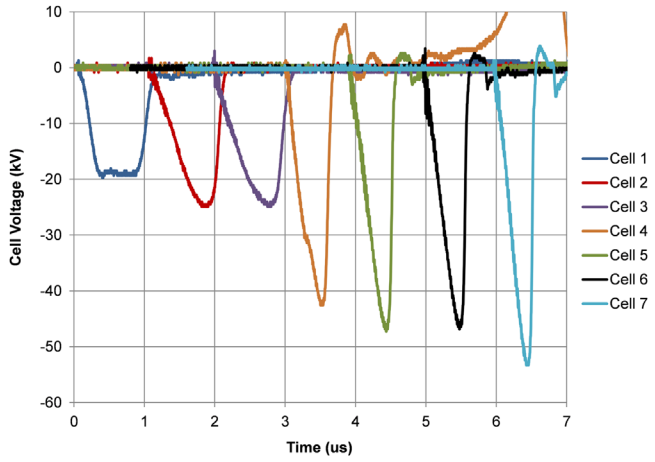

Fig. 10. Initial cell voltage waveforms produced by the compression pulsers for active cells 1–7 (from left to right). The peak output voltage and relative timing shown is arbitrary.

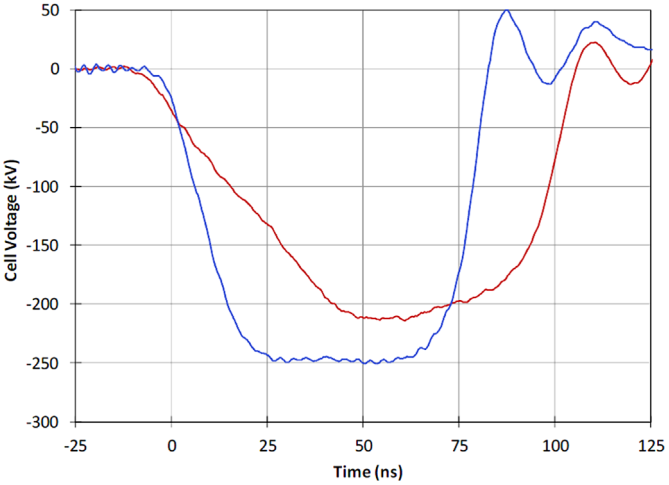

Fig. 11. Cell voltage waveforms produced by the Blumleins. The flattop voltage waveform is blue and the ramped voltage waveform is red.

utilized as 1:1 current transformers. A resistor across the cell high voltage feed is used to adjust the signal amplitude and the intrinsic L/R time constant of the diagnostic. This diagnostic is simple to calibrate with a known current source and can be used

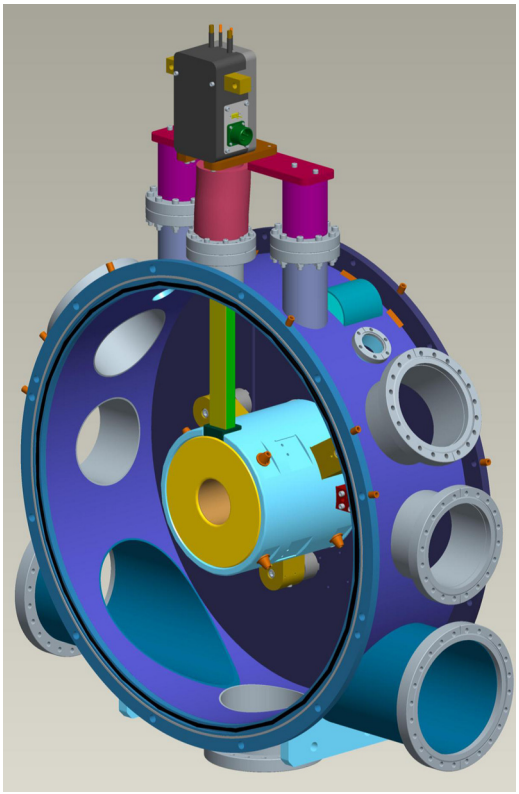

Fig. 12. Diagnostic cell CAD model.

to check the calibration of other current diagnostics. During commissioning, an end station with intercepting beam diagnostics is employed which includes a full-beam Faraday cup, 100 μm thick alumina scintillator, slit/cup beam phase space diagnostic, and a pepper pot emittance analyzer.

7. Controls, timing, and data acquisition

The control system is a distributed client/server design, utilizing National Instruments LabVIEW as the primary software development system. The system is composed of multiple data acquisition computers and network enabled industrial I/O hardware, which publish the acquired data on the local network. Higher level control, as well as archiving functions, are implemented by several workstations which interface to the acquisition system via the local network. LabVIEW's shared network variable middleware is used for all intrasystem communication. Data archiving is implemented using an Apache Cassandra cluster with a custom LabVIEW interface server.

The timing system is designed to produce all required signals in a single hardware tree, initiated by a single software or external trigger. The system is synchronized utilizing a distributed 10 MHz timing reference. A chain of commercial delay pulse generators synchronized to the master reference creates all the control triggers necessary to operate the accelerator.

Power supply control and other slow control functions are implemented by a combination of industrial and medium performance network I/O. Systems which require continuous operation, such as the vacuum system, are implemented with industrial PLC's and stand-alone loop controllers. These stand-alone systems are supervised by LabVIEW, but are capable of independent operation to ensure equipment safety. Personnel protection is implemented with a completely independent relay-based interlock system.

Data archiving and all save/restore functions depend on the open source Apache Cassandra database. The system is implemented on a small cluster of Linux virtual machines, and interfaces to LabVIEW via a custom TCP/IP server which serves to isolate the two systems. This isolation allows independent upgrade and scaling for LabVIEW and Cassandra. In addition, external access to newly acquired data will be implemented entirely through Cassandra's interfaces, keeping the LabVIEW control logic as simple as possible and accessible with free tools from the open-source community.

8. Facilities

Conventional facilities are required to support operation of the injector, accelerator, and pulsed power systems. For the pulsed power systems and the induction cells, there is a recirculating oil system which includes multiple stages of filtering and degassing to maintain the high voltage insulating properties of the Shell Diala AX oil. For the Blumleins which use water as the dielectric, there is a deionizing water system which maintains the resistivity of the water at 18 Mohm-cm. For the spark gaps in the compression pulsers and the Blumleins, there is a pressurized air system which filters, dries, and compresses air up to a maximum of 175 psig. The pressurized air is then distributed to pairs of pressure and flow regulators which provide remote control for each spark gap. Low conductivity water (LCW) is required for the solenoid and vacuum system cooling. Approximately 500 kVA of power is available for the facility and future upgrades. Turbo pumps and cryopumps maintain the average beamline pressure in the mid 10^{-7} Torr range.

9. Plans and upgrades

After commissioning the full 27-cell accelerator, a 1.2 m long plasma-neutralized drift compression line will be added beyond the last induction cell, and measurements of the compressed beam will be made. These plasma sources include ferroelectric plasma sources developed and fabricated by the Princeton Plasma Physics Laboratory and cathodic arc plasma sources in the target chamber developed by LBNL [25,26]. The existing 8.5 T final focus solenoid and target chamber from NDCX-I will be used for the initial target experiments until an upgraded target chamber is available.

The present infrastructure allows for an additional 10 accelerator cells to bring the beam energy to 3 MeV, thus broadening the range of accessible target heating experiments [3,4]. Additional accelerator cells also add beamline configuration flexibility to optimize beam compression and achieve shorter pulse lengths.

Acknowledgment

This work was performed under the auspices of the U.S. Department of Energy by LBNL under Contract DE-AC02-05CH11231.

References

[1] J.J. Barnard, et al., Nuclear Instruments and Methods in Physics Research A 606 (2009) 134.
[2] F.M. Bieniosek, et al., Ion-beam-driven warm dense matter experiments, IFSA 2009, Journal of Physics Conference Series 244 (2010) 032028.
[3] L.R. Grisham, Physics of Plasmas 11 (2004) 5727.
[4] J.J. Barnard, et al., Nuclear Instruments and Methods in Research A (2013), in this issue.
[5] P.K. Roy, et al., Physical Review Letters 95 (2005) 234801.
[6] J.E. Coleman, et al., Bunching and focusing of an intense ion beam for target heating experiments, in: Proceedings of 2007 Particle Accelerator Conference, 2007, pp. 3516–3518 .
[7] F.M. Bieniosek, et al., Nuclear Instruments and Methods in Physics Research A 606 (2009) 146.
[8] P.A. Seidl, et al., Nuclear Instruments and Methods in Physics Research A 606 (2009) 75.
[9] A. Friedman, et al., Physics of Plasmas 17 (2010) 056704.
[10] L.L. Reginato, IEEE Transactions on Nuclear Science 30 (4) (1983) 2970.
[11] A.I. Warwick, IEEE Transactions on Nuclear Science 32 (5) (1985) 1809.
[12] P.K. Roy, et al., Review of Scientific Instruments 82 (2011) 013304.
[13] P.A. Seidl, et al., Physical Review Special Topics—Accelerators and Beams 15 (2012) 040101.
[14] J.H. Takakuwa, et al., Design and fabrication of the lithium beam ion injector for NDCX-II, in: Proceedings of 2011 Particle Accelerator Conference, 2011, pp. 2032–2034.
[15] T.C. Sangster, et al., Nuclear Instruments and Methods in Physics Research A 464 (2001) 610.
[16] Rexolite (1422) is cross-linked polystyrene and is a product of C-Lec Plastics.
[17] D.G. Nilson, et al., ETA-II Accelerator Upgrades, in: Proceedings of the 1991 Symposium on Fusion Engineering, vol. 2, 1991, pp. 1179–1182.
[18] M. Burns, et al., Cell design for the DARHT linear induction accelerators, in: Proceedings of the 1991 Particle Accelerator Conference, 1991, 2958–2960.
[19] Y.-J. Chen, Nuclear Instruments and Methods in Physics Research A 292 (1990) 455.
[20] D.P. Grote, Nuclear Instruments and Methods in Research A (2013), in this issue.
[21] D. Arbelaez et al., Magnetic alignment of pulsed solenoids using the pulsed wire method, in: Proceedings of 2011 Particle Accelerator Conference, 2011, pp. 2087–2089.
[22] W.L. Waldron, Design and Fabrication of the transport solenoid pulsers for the NDCX-II induction accelerator, in: Proceedings of the 2010 Power Modulator and High Voltage Conference, 2010, pp. 251–253.
[23] W.M. Sharp, et al., Nuclear Instruments and Methods in Physics Research A 606 (2009) 97.
[24] W.L. Waldron, et al., NDCX-II pulsed power systems and induction cells, in: Proceedings of the 2009 Pulsed Power Conference, 2009, pp. 378–381.
[25] E.P. Gilson, et al., Laser and Particle Beams 30 (Issue 3) (2012) 435.
[26] A. Anders, et al., Journal of Applied Physics 91 (2002) 4824.